ON THE DEVELOPMENT OF A THEORETICALLY BASED, STATISTICALLY JUSTIFIED, THORACIC INJURY CRITERION

J. Quinn Campbell
Rabih E. Tannous
AASA, Inc.
Erik G. Takhounts
Peter Martin
Rolf Eppinger
National Highway Traffic Safety Administration
Thuvan Nguyen
CSMI Inc.

ABSTRACT

Advanced crash test dummies are being designed with multiple deflection measuring capabilities in the thorax to allow better characterization of the chest's local response to impact and thus, better optimization of performance from systems such as belt/bag combinations or four-point restraints. Historically, the injury criteria used to interpret thoracic impact responses were derived empirically from simple parameters, such as peak acceleration and deflection, that were extracted from available experimental data. This study takes a different approach. It combines the vast knowledge of structural responses and interactions embodied in our finite element modeling technologies in a model of the thorax, validates the model's impact response capability by mimicking the experiments by Kroell et al. (1972) and demonstrates that applying the measured x-y deformation-time histories of two points on the anterior chest wall of a dummy to the model, is sufficient for the model to accurately reproduce the complete two-dimensional deformation shape of the entire thoracic slice. This then allows the potential for the prediction of injury to be made on the basis of local stresses and strains occurring throughout the entire slice over time. Discussion of the development and validation of the slice model concept of post processing of dynamic dummy response output using FE models, verification of minimum necessary dummy inputs, and validation of predictive capabilities are all presented.

INTRODUCTION

Thoracic injuries are ranked second only to head injuries for automobile collisions in three categories: area most often injured (Ruan et al., 2003), overall number of fatalities and serious injuries (Cavanaugh, 1993), and overall societal harm (Malliaris, 1985). Injuries to the thorax were found to account for approximately 13% of all AIS 1-2 injuries and 29% of all AIS 3-6 injuries (Ruan et al., 2003). A better understanding of the mechanisms involved in these thoracic injuries will lead to improved restraint systems that have the ability to reduce injuries and save lives.

Thoracic injuries occur in the presence of numerous contributing factors, such as crash speed and intrusion, as well as the presence of restraint systems, including airbags, seatbelts, load limiters, and seatbelt pretensioners. While experimental research using cadavers and crash test dummies is an important step to understanding thoracic injury mechanisms, computer models offer increased flexibility at a lower cost. Computer models also offer more detailed observations of stress and strain than are possible with cadavers and test dummies. The information from chest deflection and spine acceleration can be used to calculate many thoracic injury criteria, but they do not provide much guidance in how to improve a design. The flexibility and increased measurement possibilities allow researchers to pinpoint what dummies need to measure, which will improve the ability to regulate more effectively.

In order to design more effective restraint systems and improve regulations, researchers must be able to investigate "what if" scenarios, not just focus on passing a specific metric. In fact, focusing on a single metric could lead someone in the wrong direction. Instead of a specific metric, computer models provide a variety of outcome measures which are all related to injury risk. This paper presents a 2-D finite element model of the human thorax designed to study injury mechanisms and restraint conditions in an automotive crash environment.

METHODS

The purpose of this study was to create a finite element model of the human thorax with which to study injury mechanisms under different restraint conditions, and use the model in conjunction with multiply measured thoracic deflection time-histories obtained on THOR, the advanced frontal impact dummy developed by the NHTSA, to predict injury. The complexity of the model was determined by balancing computational issues, such as including enough complexity to accurately represent the response of the thorax while still maintaining a relatively fast run time on a PC. For this purpose, a 2D model was selected over a 3D model. After creating the mesh for the 2D thorax, the model's response was validated against thoracic impact experiments. Once the model was validated,

simulations were run to test the response of the model under various restraint conditions. Specifically, the model was tested to determine if it can differentiate between the concentrated loading condition of a torso belt from the distributed loading condition of an airbag. Next, applied displacements were used to replicate the restraint loading and determine if points corresponding to the THOR crux points, i.e., those sights on the anterior chest wall where deflection sensing instrumentation is attached, were sufficient to replicate the simulations. Finally, simulations were conducted to correlate stresses and strains in the model to injury. A large set of cadaveric impact tests were used to derive and apply displacements to the model corresponding to THOR crux points. A variety of model outputs were analyzed and a criterion was developed to predict injury.

Model Description

The finite element model of the thorax was modeled using the LS-Dyna software package. The model represents a 50th percentile male thorax. As previously stated, it was created in two dimensions to allow simulation of the overall thorax response while dramatically reducing the solution time. The thorax model (Figure 1) contains six parts: rib, sternum, viscera, elastic spine, rigid spine, and spine/rib joint.

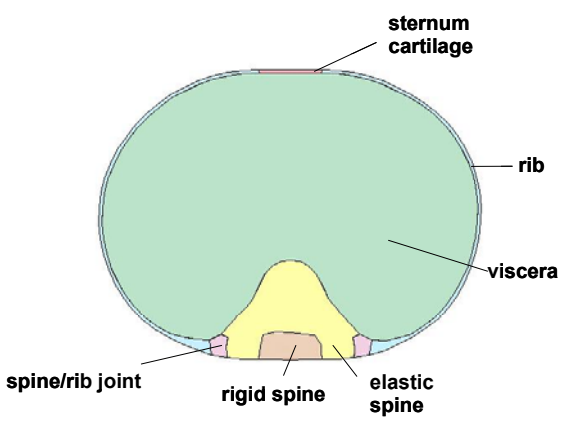

Figure 1. 2-D Thorax Finite Element Model.

The material properties for the model are shown in Table 1 and were determined through a review of the literature. A variety of material models were considered and tested for the deformable parts in the model, including elastic, viscoelastic, and piecewise linear plasticity models. The piecewise linear plasticity material was used because it provided the most biofidelic behavior when tested. This material scales the yield stress based on the strain rate as shown in equation 1:

$$\sigma_y(\varepsilon^p_{eff}, \varepsilon'^p_{eff}) = \sigma^s_y(\varepsilon^p_{eff}) + SIGY*(\varepsilon'^p_{eff}/C)^{(1/p)} \quad (1)$$

where $\sigma_y(\varepsilon^p_{eff}, \varepsilon'^p_{eff})$ = effective stress, $\sigma^s_y(\varepsilon^p_{eff})$ = static stress, SIGY = yield stress, ε'^p_{eff} = strain rate, and C and p are user defined coefficients (LS-Dyna User's Manual, 2003).

Table 1.
Material Properties of the thorax finite element model, (Granik and Stein, 1972, Deng, 2000).

Part Name	Density (kg/m^3)	Stiffness (kPa)	Yield Stress (kPa)
Sternum	2.5e-6	1200000	3445
Rib	1.1e-6	10335000	85284
Viscera	2.9e-6	207	0.69
Spine/Rib Joint	1.1e-6	1200000	3445
Elastic Spine	1.1e-6	25982190	N/A
Spine (rigid)	1.1e-6	rigid	N/A

The rib properties required some modification because the model is two-dimensional. Specifically, the space between the ribs in the full thorax cannot be directly modeled in two dimensions. The stiffness of the thorax is dependent on the total cross-sectional area of ribs in the thorax. An extruded 2-D thorax model would have one solid rib without any space between ribs, making the model too stiff. Therefore, to ensure the proper response of the model, the cross sectional area of the rib in the model was reduced to account for the space between the ribs, while the rib modulus was kept constant. First, an average rib cross sectional area was determined to be 0.73 cm2 (Pintar & Yoganandan, 1998). A rectangular cross section was assumed with a height of 1.27 cm and a thickness of 0.58 cm. Next, the average sternum length, from rib 1 to rib 10, of a 50th percentile male was found to be 29 cm (Robbins, 1983). Based on the average cross section the ribs should take up 7.3 cm2 leaving 9.52 cm2 space between the ribs. Therefore, the ribs take up 44% of the area. To account for the space between the ribs, the cross sectional area of the rib in the 2-D model should be 44% of the average rib. The thickness of the rib in the 2-D model was reduced to a thickness of 0.25 cm; with a height of 1.27 cm the rib has a cross sectional area of 0.32 cm2.

The mass of the model was determined by comparing the mass and area of the full thorax to the mass and area of the 2-D thorax model. The mass of a 50th percentile male is 76.3 kg, with a thorax mass

of 23.6 kg (Robbins, 1983). The contact area on the 3-D thorax is 161 cm2 (Kroell, 1974) and the contact area of the 2-D thorax is 18 cm2. Therefore, the mass of the 2-D thorax was determined by multiplying the full thorax mass by the ratio of the thorax areas as shown in equation 2, resulting in a 2-D mass of 2.7 kg.

$$\text{2-D Mass} = \text{3-D Mass} * (\text{2-D Area} / \text{3-D Area}) \quad (2)$$

Model Validation

Fourteen experimental tests from Kroell et al., 1971 and 1974 (shown in Table 2) were simulated to validate the response of the thorax model under impact. These included ten free back tests and four fixed back tests. For the simulation of the fixed back tests, the rigid spine was restrained in all directions. Four of the free back tests had the skin on the thorax removed. For each simulation, the model was scaled based on the size and mass of the cadaver for that test. Each test was simulated using a representation of a 15.2 cm diameter impactor with the same initial velocity as in the experiments. The impactor was modeled as two-dimensional and its mass was scaled in the same manner as the mass of the model, based on the ratio of the 3-D and 2-D surface areas (Equation 2). Only initial conditions were provided, and each simulation then proceeded forward in time according to the laws of mechanics.

The results of each simulation were evaluated using force displacement curves, force time histories, and displacement time histories. Because the simulations used a 2-D model with scaled down masses, the forces in the simulation had to be scaled back up before they were compared to the experimental data. It should also be noted that a different scale factor was used for the tests that had the skin on the thorax removed than for the tests that did not. An assumption was made that the tests in which the skin on the thorax was intact would have a contact area that included the entire surface of the impactor (161 cm2), due to the skin's distribution of the load to the underlying structures. In contrast, the tests with the skin removed will have a lower contact area (105 cm2) because the impactor force will only be distributed over the ribs and sternum, and not the interstices. The force scale factors were calculated using the ratio of the 3-D contact area to the 2-D contact area (18 cm2 in both cases). Therefore, the scale factor for the tests with the skin intact was 8.8 and the scale factor for the tests with skin removed was 5.8.

Table 2.
List of Tests Simulated for Validation * = Fixed Back Test, ** = Skin Removed.

Test No	Initial Velocity (kph)	Impactor Mass (kg)	Chest Depth (cm)	Cadaver Mass (kg)
92	48	1.6	18	41
96	30	19	24	59
99	26	19	23	75
104	35	23	25	74
171	18	23	22	55
177	18	23	25	64
182*	25	10	23	65
186*	26	10	23	60
187*	24	10	25	82
188*	26	10	22	52
7**	14	19	20	38
10**	18	19	19	43
6**	19	19	25	77
5**	19	19	26	86

Restraint Combination Simulations

Thirty simulations were run to test the 2-D thorax model's performance under different loading combinations of hypothetical restraint systems. Loads were applied to the model to simulate either pure airbag loading, seatbelt loading, or a combination of the two. Airbag loading was distributed evenly over the chest anterior surface as shown in Figure 2, while concentrated seatbelt loading was at an angle of 25 degrees and distributed across three adjacent nodes with 44% of the load applied on the center node and 28% on each side. Two seatbelt positions were simulated (Figures 3 and 4): a center position to simulate where the seatbelt crosses at the upper thorax (near rib 4) and a lateral position to simulate where the belt crosses the lower thorax (near rib 8). In all of the simulations the rigid spine was allowed to translate in the x and y directions but no rotation was allowed.

Loading was applied as a triangle pulse starting at 0, reaching 100% of the applied load at 100 ms, and returning to 0 again at 125 ms. A base loading level was assumed at a force level that resulted in a reasonable chest deflection and 50 m/s^2 spine acceleration. Three different total loading levels were simulated by applying the force across three adjacent nodes: 125%, 100% and 75% of the base loading level. The sum of the airbag and seatbelt loads resulted in the total load specified for

that simulation. The list of the various simulation loading combinations is provided in Table 3.

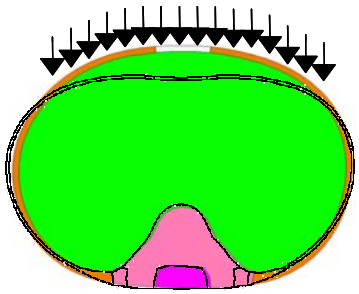

Figure 2. Distribution of Airbag Only Loading.

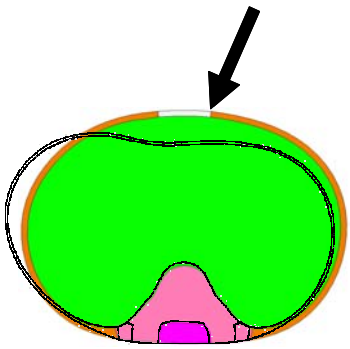

Figure 3. Location of Center Position Seatbelt Loading.

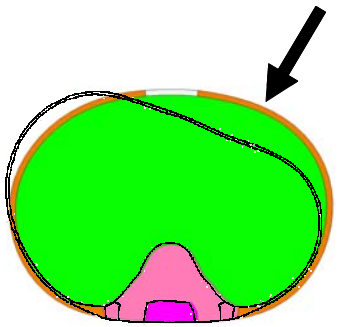

Figure 4. Location of Lateral Position Seatbelt Loading .

Table 3.
List of Tests in Restraint Combination Simulations.

Test No	Total Load	Belt Position	% Belt Loading	% Airbag Loading
1	100%	Center	100%	0%
2	100%	Center	75%	25%
3	100%	Center	50%	50%
4	100%	Center	25%	75%
5	100%	Center	0%	100%
6	125%	Center	100%	0%
7	125%	Center	75%	25%
8	125%	Center	50%	50%
9	125%	Center	25%	75%
10	125%	Center	0%	100%
11	75%	Center	100%	0%
12	75%	Center	75%	25%
13	75%	Center	50%	50%
14	75%	Center	25%	75%
15	75%	Center	0%	100%
16	100%	Lateral	100%	0%
17	100%	Lateral	75%	25%
18	100%	Lateral	50%	50%
19	100%	Lateral	25%	75%
20	100%	Lateral	0%	100%
21	125%	Lateral	100%	0%
22	125%	Lateral	75%	25%
23	125%	Lateral	50%	50%
24	125%	Lateral	25%	75%
25	125%	Lateral	0%	100%
26	75%	Lateral	100%	0%
27	75%	Lateral	75%	25%
28	75%	Lateral	50%	50%
29	75%	Lateral	25%	75%
30	75%	Lateral	0%	100%

Applied Crux Simulations

To determine how well the deformation of the slice model induced by the variety of force/area/time profiles discussed above can be duplicated by having only knowledge of the THOR's two x-and-y CRUX displacement time histories as the model's stimulus, the previous simulations were rerun by applying only the calculated CRUX displacements obtained from the previous calculations force stimulated simulations. Sixty additional simulations were conducted; two tests were run for each of the tests in Table 3, one with applied upper crux displacements, one with applied lower crux displacements. In each test the spine was fixed in all directions. The simulations with applied displacements were then compared to the original simulations using applied forces and the respective deformations, stresses, and strains compared.

Injury Correlation

To answer the question "How similar would the deformation of the thorax cross section be if, rather than loading the thoracic slice model with a particular force, area, time history, one only used the two dimensional (x,y) displacements of the anterior CRUX measurement points that the force-area-time loading produced," 54 frontal impact cadaver sled tests were selected from the NHTSA database. The upper chestband data was processed for each test by a program written to derive the x and y displacements of points corresponding to the THOR crux points relative to the spine. The initial points were chosen based on which points were closest to the THOR crux points based on the x distance from the sternum. Once the initial points were selected, the x and y displacement time histories for each point were used as load curves for the thorax model. A simulation was run for each test based on the upper crux displacements. Each simulation was analyzed and processed to output peak stresses and strains during the simulation. Next, logistic regression was performed to correlate the injuries found in the sled tests to the outputs of the model. Injury in the sled tests was determined by the number of rib fractures found. Regressions were performed with injury thresholds at 2-6 rib fractures to determine the best cutoff point for injury. Regressions were also performed by correlating either only upper thoracic fractures (ribs 1-5) or fractures for the full thorax. While 54 tests were initially chosen, the number of tests for each regression varied depending on the quality control of chestband data and if the tests had full reports to determine upper from lower rib fractures.

RESULTS

Model Validation

Each test in Table 2 was simulated using the slice model and the experimentally observed peak displacements and forces were compared with those predicted by the model. Figures 5 and 6 illustrate results for peak displacement and force respectively. Figures 7 through 13 illustrate comparisons of individual simulated and experimentally observed force-time, displacement-time, or force-displacement/displacements from representative tests. Examples are given for each type of test: free back with skin, free back without skin, and fixed back. Time histories for the tests without skin are not shown because the experimental data was not available.

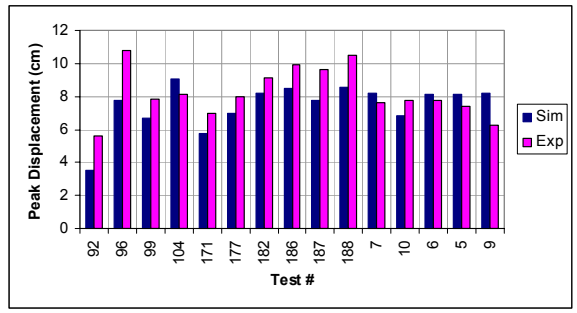

Figure 5. Comparison of Peak Displacements.

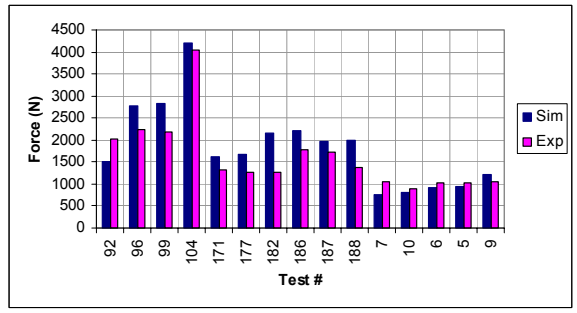

Figure 6. Comparison of Peak Forces.

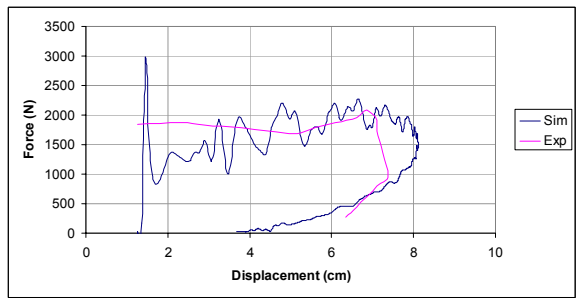

Figure 7. Force Displacement Curve, Test 7, Free Back Without Skin.

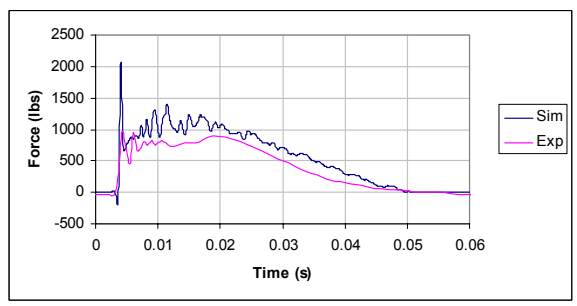

Figure 8. Force Time History, Test 99, Free Back With Skin.

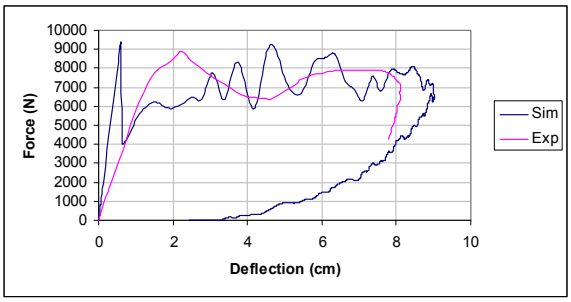

Figure 9. Force Displacement Curve, Test 104, Free Back With Skin.

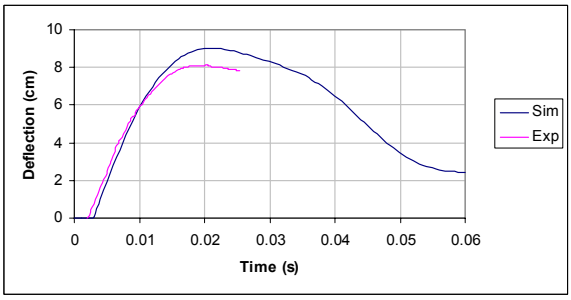

Figure 10. Displacement Time History, Test 104, Free Back With Skin.

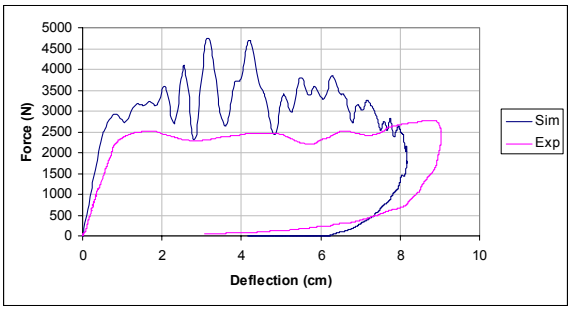

Figure 11, Force Displacement Curve, Test 182, Fixed Back With Skin.

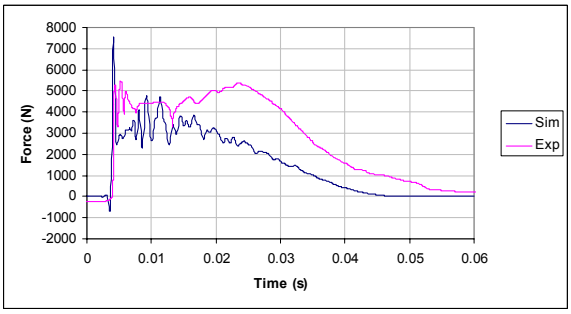

Figure 12. Force Time History, Test 182, Fixed Back With Skin.

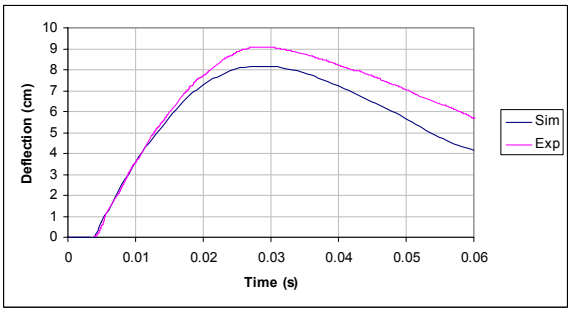

Figure 13. Displacement Time History, Test 182, Fixed Back With Skin.

Restraint Combination Simulations

Each loading condition described in Table 3 was simulated using the slice model and the x and y displacements of the two upper and two lower anterior THOR crux points to determine a maximum stress and strain in the rib. Examples are shown comparing the different test conditions: restraint combinations, belt positions, and loading levels (Figures 14-19). Figures 14, 16, and 18 present the initial position and maximum displacement of the anterior crux points with respect to the spine under the various force loading conditions.

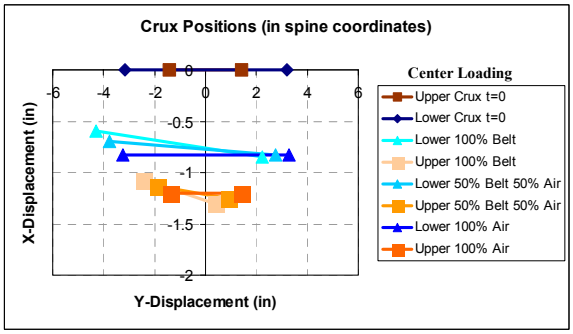

Figure 14. Comparison of Crux Displacements for Different Restraint Combinations.

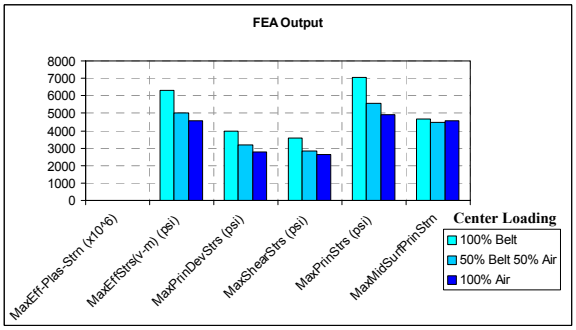

Figure 15. Comparison of Rib Stress and Strain for Different Restraint Combinations.

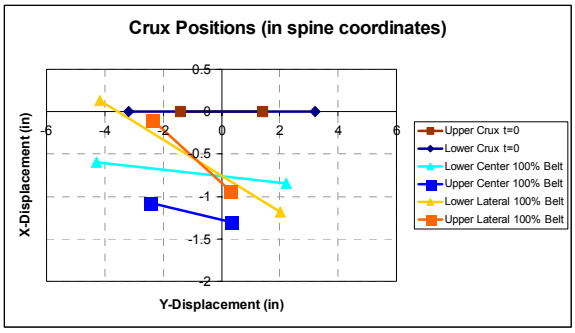

Figure 16. Comparison of Crux Displacements for Different Belt Positions.

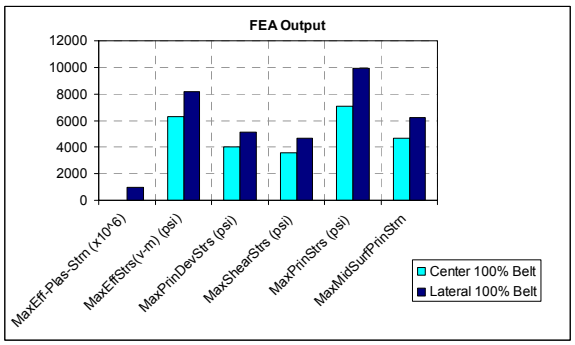

Figure 17. Comparison of Rib Stress and Strain for Different Belt Positions.

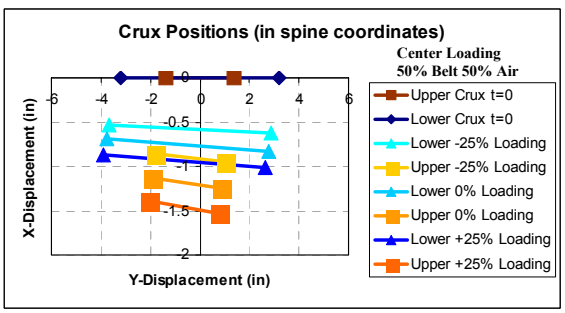

Figure 18. Comparison of Crux Displacements at Different Loading Levels.

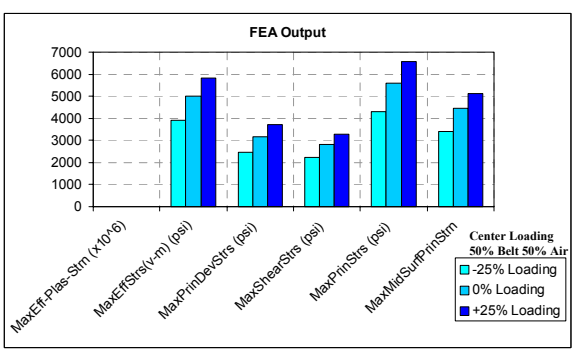

Figure 19. Comparison of Rib Stress and Strain at Different Loading Levels.

Applied Crux Simulations

Each test in Table 3 was also simulated using only applied upper or lower crux displacements obtained from the previous 30 tests just discussed. All tests were processed to compare the overall deformation of the displacement-stimulated model with the deformation of the force stimulated model. Good replication of deformation shape was noted. The following charts provide a comparison between the original loading simulations, applied upper crux simulations, or applied lower crux simulations (Figures 20-23). Due to limited space, examples are shown only for select restraint combinations.

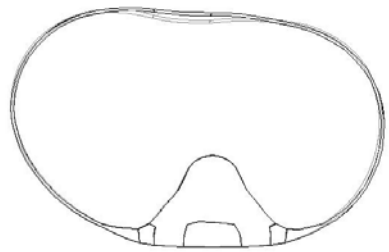

Figure 20. Overlay showing both the original loading (grey) and applied lower crux (black) rib contours for the 100% center belt loading condition.

These results strongly suggest that post processing THOR generated upper and lower chest deflections using the slice model can provide a reasonable estimate of the stress/strain distributions found in a force deformed thorax and the potential for damage/injury throughout the entire event. To investigate this further, the slice model was displaced by applying the two crux displacement time histories obtained when conducting the kinetic force applications previously discussed and the error between the two stresses compared.

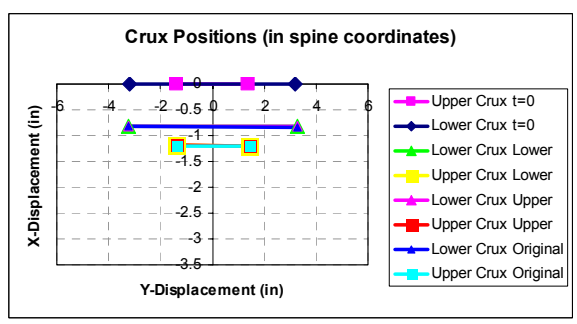

Figure 21. Comparison of Crux Positions for 100% Airbag Loading.

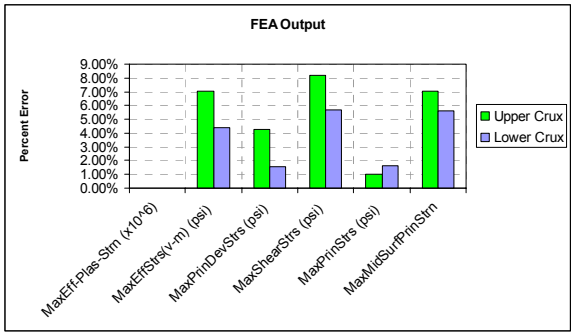

Figure 22. Comparison of Error in Rib Stress and Strain for 100% Airbag Loading.

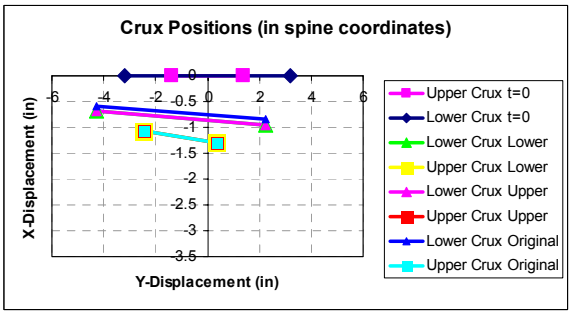

Figure 23. Comparison of Crux Displacements for 100% Center Belt Loading.

Injury Correlation

The 54 frontal impact cadaver sled tests were simulated using the slice model and chestband data from each experimental test. Each simulation was analyzed and processed to output peak stresses and strains seen in the slice model during the simulation. Logistic regressions were performed to correlate the injuries found in the sled tests to the outputs of the model. An example of the rib contours at peak deflection from the chestband alone and upper crux simulation using only crux displacements for test 2910 is shown in figure 24.

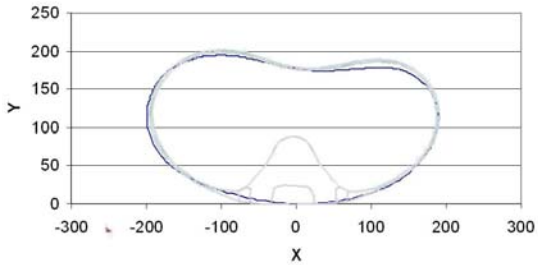

Figure 24. Rib contours at peak deflection from test 2910, upper crux simulation (grey), cadaver chestband (black).

Numerous logistic regressions were performed on the data from the chestband simulations: using different outputs from the simulations, injury thresholds from 2-6 rib fractures, and separate correlations for upper rib fractures versus all rib fractures. Various confounding variables were tested in the regressions as well, including cadaver age, weight, and sex. The regression with the most significance (p-value 0.0001) and highest Chi2 (18.0) used maximum principal strain from the upper crux simulation with cadaver age to predict injury defined as greater than 2 rib fractures in the entire thorax. 84% of the tests used in the regression had correct prediction of injury using the model (ROC=0.84). Figure 25 shows the probability of injury for this model at different ages.

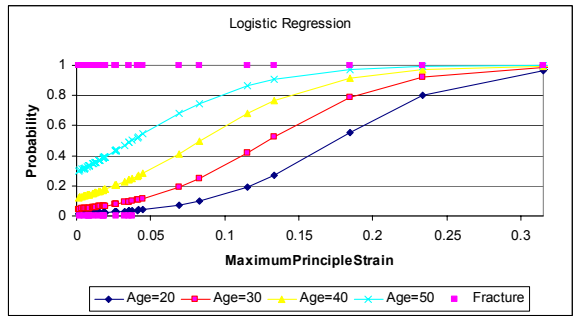

Figure 25. Logistic Regression with injury defined as greater than 2 rib fractures.

DISCUSSION

Model Validation

The 2-D finite element model of the thorax shows reasonable correlation with the impact experiments of Kroell et al. The force displacement curves and time histories show that the model has a biofidelic response through the entire event, including at the peaks. The force scaling methods seem to allow accurate comparison of 3-D and 2-D force measurements. This is demonstrated in the accurate simulation of cases with and without skin. However, overall the results suggest that the model may be too stiff based on slightly higher forces and lower displacements seen throughout the simulations. It is possible that these results could be improved by altering the average rib cross section that was used, since the cross section of ribs varies greatly both along their length and at different levels within the thorax. Overall, the model performs relatively well in both fixed and free back conditions and the model can be used to evaluate restraint conditions with seatbelts and/or airbags.

Restraint Combination Simulations

The thirty simulations using various combinations of airbag and seatbelt loading, various seatbelt positions, and three loading levels, showed that the 2-D thorax model can appropriately differentiate between different restraint systems. A comparison of the belt positions in Figure 17 shows that lateral belt loading is more severe than center belt loading, 100% lateral belt loading being the most severe condition tested. Figure 19 shows that increasing the overall load results in higher stresses and strains, as expected. Figure 15 shows that the 100% belt loading condition results in higher stresses and strains than either combined loading or airbag loading. 100% airbag loading had the lowest stress and strain levels of any restraint combination. Logistic regression showed that all of the stress components examined had the ability to differentiate the 100% seatbelt condition from the others (p=0.003-0.002), while the maximum effective plastic strain and the maximum principal strain had less ability to differentiate the restraint conditions, p=0.024 and p=0.154 respectively. The ability for the 2-D thorax model to differentiate seatbelt loading from other types of restraint conditions is an important ability because field research has shown seatbelt only restraints to be more likely to produce injuries (Trosseille et al., 2001).

Applied Crux Simulations

The results from the applied crux simulations show that in general the model has the ability to replicate the contours, stresses, and strains in a variety of loading conditions using only the planar (x,y) displacements of two crux points. However, the simulations show that with increased loading levels and/or increased belt loading the error increases between the applied crux simulations and the original simulations. Also, the results show that the belt position affects the ability for the applied crux simulations to replicate the loading. When upper crux displacements are applied there is more error in the lateral belt loading position, while when the lower crux displacements are applied there is more error in the center belt loading position. This is a result of the upper crux points being close to the center of the chest while the lower crux points are spread out more laterally. Figure 26 shows the error in maximum principal Von Mises stress for each simulation. While there is some error when simulating thoracic loading with applied crux displacements, the contours and stresses are close enough to provide useful information that isn't available from the crux displacements alone. Therefore, using the 2-D thorax model in conjunction with THOR makes it a useful research tool to differentiate differences in restraint performance.

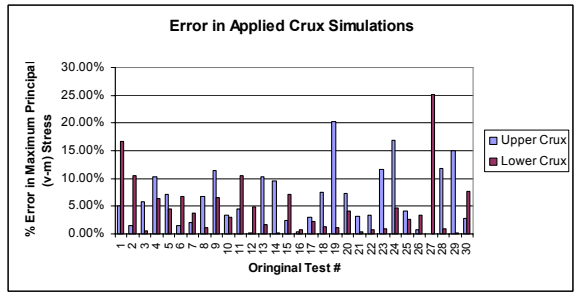

Figure 26. Error in Von Mises Stress for Applied Crux Simulations.

Injury Correlation

The results from the simulations of the cadaver tests showed that the best model for predicting injury used maximum principal strain from the simulations with cadaver age as a confounder. This model is promising because maximum principal strain is physically linked to fracture. The ability for the model to predict injury accurately in 84% of the tests shows the models ability to differentiate injury from non-injury. One potential problem with the model is that at high ages it is very unlikely to predict non-injury, even at low strains. This may be due to limits of the analysis techniques used or the nature of the test data available and may be remedied using the full rage of available tests.

CONCLUSIONS

- The 2-D finite element model of the thorax correlates well to the impact experiments of Kroell et al.
- The force scaling methods seem to allow accurate comparison of 3-D and 2-D force measurements.
- The model has a biofidelic response through the entire impact event, including at the peaks.
- The model performs relatively well in both fixed and free back conditions.
- The model can be used to evaluate restraint conditions with seatbelts and/or airbags.
- The model has the ability to differentiate belt loading from other restraint conditions based on higher stresses and strains.

- Upper or lower THOR crux displacements can be applied to the 2-D thorax model to replicate loading simulations.
- A logistic regression model using maximum principal strain and age has a high probability of predicting thoracic injury.

REFERENCES

[1] CAVANAUGH, J. (1993) The biomechanics of thoracic trauma. In Accidental Injury Biomechanics and Prevention, ed. A. Nahum and J. Melvin, pp. 362-390. Springer-Verlag, New York.

[2] DENG, Y.C. and CHANG, F. (2000) F8B: Development of A Finite Element Human Thorax Model, Final Report. GM North America Car Group.

[3] GRANIK, G and STEIN, I. (1973) Human ribs: static testing as a promising medical application. J Biomech. May;6(3):237-40.

[4] KROELL, C.K., SCHNEIDER, D.C., NAHUM, A.M. (1971) Impact Tolerance and Response of the Human Thorax. Proc. 15th Stapp Car Crash Conference, pp 84-134. Society of Automotive Engineers, Warrendale, PA.

[5] KROELL, C.K., SCHNEIDER, D.C., NAHUM, A.M. (1974) Impact Tolerance and Response of the Human Thorax II. Proc 18th Stapp Car Crash Conference, pp 383-412. Society of Automotive Engineers, Warrendale, PA.

[6] LS-DYNA Keyword User's Manual (2003) Vol I and II, Version 960, Livermore Software Technology Corporation, Livermore, CA.

[7] MALLIARIS, A. C., et al. (1985) Harm causation and ranking in car crashes. Paper 8500090, Society of Automotive Engineers, Warrendale, PA.

[8] YOGANANDAN, N. and PINTAR F.A. (1998) Biomechanics Of Human Thoracic Ribs. J Biomech Eng. Feb;120(1):100-4.

[9] ROBBINS, D.H. (1983) Anthropometric Specifications for Mid-Sized Male Dummy. UMTRI Report Number 83-53-2, Anthropometry of Motor Vehicle Occupants. Volume 2 - Mid-Sized Male. U.S. Department of Transportation. National Highway Transportation Safety Administration.

[10] RUAN, J., EL-JAWAHRI, R., CHAI, L., BARBAT, S., PRASAD, P. (2003) Prediction and Analysis of Human Thoracic Impact Responses and Injuries in Cadaver Impacts Using a Full Human Body Finite Element Model. Proc. 47th Stapp Car Crash Conference, pp. 299-321. Society of Automotive Engineers, Warrendale, PA.

[11] TROSSEILLE, X., FORET-BRUNO, J-Y., PAGE, Y., HUERE, J-F., LE COZ, J-Y., BENDJELLAL, F., DIBOINE, A., PHALEMPIN, T., VILLEFORCEIX, D., BAUDRIT, P., GUILLEMOT, H., and COLTAT, J-C. (2001) Comparison of Thoracic Injury Risk in Frontal Car Crashes for Occupant Restrained Without Belt Load Limiters and Those Restrained With 6kN and 4kN Belt Load Limiters. Proc. 45th Stapp Car Crash Conference, pp. 205-224. Society of Automotive Engineers, Warrendale, PA.